

# Spectral Quality Metrics for VNIR and SWIR Hyperspectral Imagery\*

John P. Kerekes<sup>#</sup> and Su May Hsu  
Sensor Technology and System Applications Group  
Lincoln Laboratory, Massachusetts Institute of Technology

## ABSTRACT

Current image quality approaches are designed to assess the utility of single band images by trained image analysts. While analysts today are certainly involved in the exploitation of spectral imagery, automated tools are generally used as aids in the analysis and offer hope in the future of significantly reducing the timeline and analysis load. Thus, there is a recognized need for spectral image quality metrics that include the effects of automated algorithms.

We have begun initial efforts in this area through the use of a parametric modeling tool to gain insight into parameter dependence on system performance in unresolved object detection applications. An initial Spectral Quality Equation (SQE) has been modeled after the National Imagery Interpretation Rating Scale General Image Quality Equation (NIIRS GIQE). The parameter sensitivities revealed through the model-based trade studies were assessed through comparison to analogous studies conducted with available data. This current comparison has focused on detection applications using sensors operating in the VNIR and SWIR spectral regions.

The SQE is shown with key image parameters and sample coefficients. Results derived from both model-based trade studies and empirical data analyses are compared. Extensions of the SQE approach to additional application areas such as material identification and terrain classification are also discussed.

Keywords: Spectral imaging, spectral quality

## 1. INTRODUCTION AND CONTEXT

The ability to quantitatively assess the quality of a multispectral or hyperspectral image is desirable for many reasons including instrument comparisons and trade studies, image archive retrieval and tasking of data collections. However, the notion of the “quality” of a spectral image will depend upon many disparate factors including characteristics of the scene, the sensor, the algorithms applied, and the desired product. While an image with just a few bands but high spatial resolution may have high quality judged by someone looking at spatial information, an image with many bands but moderate spatial resolution may have even higher quality when judged by an analyst looking at spectral information. It is precisely these tradeoffs that one seeks to quantify in the development of a spectral quality measure.

The myriad of applications of spectral imagery and the dependence of perceived quality on the interrelationships of parameters make the task of assigning a quality measure to spectral imagery very daunting. To make the problem tractable, the work described in this paper constrained the problem to a single task: unresolved object detection with a spectral matched filter in the reflective solar spectral region. This task is well suited to the automated processing of hyperspectral imagery since no visible spatial clues are available to an analyst and one must rely on the application of the detection algorithm.

---

\* This work was sponsored by the Department of Defense under contract F19628-00-C-0002. Opinions, interpretations, conclusions, and recommendations are those of the author and not necessarily endorsed by the United States Government.

<sup>#</sup> kerekes@ll.mit.edu; phone (781) 981-0805; fax (781) 981-7271; MIT Lincoln Laboratory, 244 Wood St., Lexington, MA 02420-9108

There have been other efforts at assigning a quantitative quality measure to hyperspectral imagery including ones based on analysts' interpretation of quality and utility [1] [2], spectral similarity [3], and the relationship of detection and false alarm probabilities with collection parameters [4]. These efforts offer alternative approaches to this difficult problem and demonstrate promise in the context of their work.

This paper describes our approach and initial results in developing a candidate spectral quality metric in the context of unresolved object detection. First, we discuss some of the issues regarding spectral quality and describe a notional concept of a spectral quality equation and a spectral quality rating scale. We then review the General Image Quality Equation (GIQE) that was used as a model for the proposed Spectral Quality Equation (SQE). Parameter tradeoff sensitivities are investigated using an end-to-end spectral imaging system model and then used to derive the SQE. Similar tradeoff studies were conducted using airborne hyperspectral imagery and the results presented for comparison to the model derived results. We conclude with discussions of some ideas on spectral quality and topics for further research.

## 2. SPECTRAL QUALITY PARAMETERS AND NOTIONAL CONCEPT

### 2.1 Spectral Quality Discussion

The notion of the "quality" of a multispectral or hyperspectral image deserves some discussion, as there is not a universally accepted definition of the term. In this usage, the dictionary defines quality as "degree or grade of excellence." Thus, a spectral quality measure should contain a monotonically increasing scale that represents the degree of excellence (in some sense) of a spectral image. The use of a numerical scale to describe the quality is a convenient way of ordering the values and comparing disparate images. It is intuitive that the higher the numerical value, the higher the quality.

As mentioned in the Introduction, the degree of excellence, or quality, of an image can depend on the particular use of the image. A farmer looking for signs of a non-localized disease outbreak in his crops may not be concerned whether the imagery has 5 or 10 meter spatial resolution, but rather whether it has the spectral resolution and band locations to detect the impending stress. On the other hand, a military analyst looking for small objects may be more concerned about the spatial resolution than the spectral content. Thus one must consider the application when discussing spectral image quality.

Another aspect of assigning a numerical value for the quality of a spectral image is to distinguish between potential and actual value. A spectral image may have the signal-to-noise ratio and spectral resolution to identify a crop type, but there may be a cloud present over the field of interest in the image. Thus, while the image has high potential quality, its actual utility is low for the problem of interest.

In this initial work on the topic, we have elected to constrain the application to one of sub-pixel (unresolved) *target* detection where target refers to a material, object, or localized disturbance in the natural background. Also, we will use the term quality to describe the *potential* value of the spectral image and set aside issues regarding obscuration in a given image.

### 2.2 Parameters Affecting Spectral Quality

Given the constraints we have adopted in this work, there still remain a large number of parameters of the remote sensing system that will affect the quality of the imagery. Table 1 lists a number of these parameters grouped according to their place in the end-to-end remote sensing system.

While this list is not comprehensive, it still contains many diverse parameters. Again, to make this effort tractable, we further reduce the parameters studied to the three most likely to affect quality: spatial resolution, spectral resolution, and signal-to-noise ratio (highlighted in bold in Table 1).

Table 1. Example parameters affecting spectral image quality in current context. **Bold** parameters are the focus in this work.

Scene	Target of interest (size and spectral complexity) Background class(es) and their complexity Atmospheric state Solar zenith angle
Sensor	<b>Spatial resolution</b> and sampling <b>Spectral resolution</b> and sampling Spectral region <b>Signal-to-noise ratio</b> Calibration accuracy (radiometric and spectral) Total field of view View angle
Processing Algorithms	Spectral selection and/or feature extraction Atmospheric compensation Detection algorithm

### 2.3 Spectral Quality Notional Concept

Now that we have discussed the definition, context, and parameters affecting spectral quality, let us motivate the approach we have pursued with a simple diagram as shown in Figure 1. Here, we see three axes representing the primary parameters of a spectral imaging system selected above. Ground resolved distance (GRD) represents spatial resolution. Channel spectral bandwidth, or  $\Delta\lambda$ , represents spectral resolution. Noise level is used as a surrogate for signal-to-noise ratio.

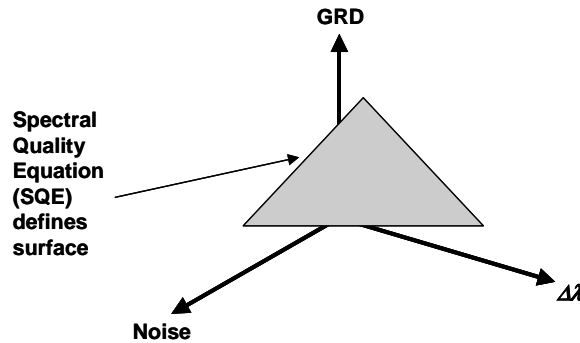


Figure 1. Notional concept of the Spectral Quality Equation defining a surface of constant quality.

Note that as one moves away from the origin in Figure 1 the values of the parameters increase and lead to a degradation of the image quality in an intuitive sense. The notional surface drawn in the figure represents the concept of tradeoffs in these parameters that lead to a constant quality level. The surface defines the concept of a spectral quality equation (SQE), which describes these tradeoffs in quantitative terms. Parameter combinations that lie on the surface described by the SQE will have equivalent quality. This concept is extended to an idea of a Spectral Quality Rating Scale (SQRS), which leads to multiple surfaces at various distances from the origin, with surfaces closer to the origin having a higher numerical value (greater quality). The SQRS is further discussed in Section 4.

### 3. REVIEW OF GENERAL IMAGE QUALITY EQUATION (GIQE)

The concept of image quality has an extensive history in the context of analyst interpretation of electro-optic (EO) panchromatic imagery [5]. In particular, the National Imagery Interpretability Rating Scale (NIIRS) [6] was developed to have a quantitative scale by which EO imagery is rated. The scale rates an image from level 0 to level 9 with increased interpretability corresponding to the higher levels. The NIIRS was developed by having a large number of trained image analysts subjectively evaluate the quality of sample EO imagery, order the imagery from least to most useful, and then overlay a quantitative scale to the ranked imagery. Subsequent to this subjective development, the sensor parameters for

a sample set of images were regressed against the NIIRS values and the General Image Quality Equation (GIQE) was generated [7]. The GIQE allows the prediction of the NIIRS rating for an image given the sensor parameters. One form of the equation is described in equation 1 as taken from [7].

$$NIIRS=10.25-3.32\log_{10}[GSD(in)]-\frac{0.34G}{SNR}+1.56\log_{10}[RER]-0.66H \quad (1)$$

where,

- GSD* – ground sample distance in inches
- SNR* – signal-to-noise ratio
- G* – noise gain term (typically ~10)
- RER* – relative edge response (typically ~0.9)
- H* – overshoot-height term (typically ~1.3)

Thus, given a set of imaging system parameters, one can use the GIQE to predict the numerical NIIRS level. The GIQE was used as a model for the SQE developed in this work.

#### 4. MODEL-BASED TRADE STUDY AND SPECTRAL QUALITY EQUATION

In order to investigate the tradeoffs between the parameters identified in Section 2 (GRD, spectral resolution, and SNR), we used an analytical spectral performance prediction model [8] that runs quickly and allows a large number of parameter combinations to be studied efficiently.

We defined a nominal observation scenario with a subpixel target object embedded within a single background, a notional airborne hyperspectral imager with spectral coverage from 0.4 to 2.5 μm, and a spectral matched filter detection algorithm using a known spectral signature. From this nominal scenario, a number of parameter combinations (3x3x33x9x4 = 10,692) were run as described in Table 2. In each case, the probability of detection at a specified probability of false alarm was calculated using the model. Note that the number of channels is used as a surrogate for spectral resolution by aggregating adjacent channels to form fewer channels from the initial 120 selected to cover the spectral region (omitting atmospheric absorption bands).

Table 2. Parameter values studied in the model-based detection tradeoff analyses.

Target object classes	Object 1, object 2, object 3
Background classes	Trees, grass, road
Target pixel fill fraction	1% to 100% in increments of 3%
Signal-to-Noise Ratio	5, 10, 25, 50, 100, 250, 500, 1000, 2000
Number of spectral channels	15, 30, 60, 120

Figure 2 shows an example result from a subset of these runs. On the left are shown the curves for a given target in a given background predicting probability of detection (at probability of false alarm = 10<sup>-5</sup>) versus subpixel target fill fraction as a function of signal-to-noise ratio. The graph on the right re-plots the same data, but after converting the pixel fill fraction to an equivalent linear ground resolved distance given a 1 square meter target. For- example, a pixel fill fraction of 25% corresponds to a ground resolved distance of 2 meters for a 1 square meter target.

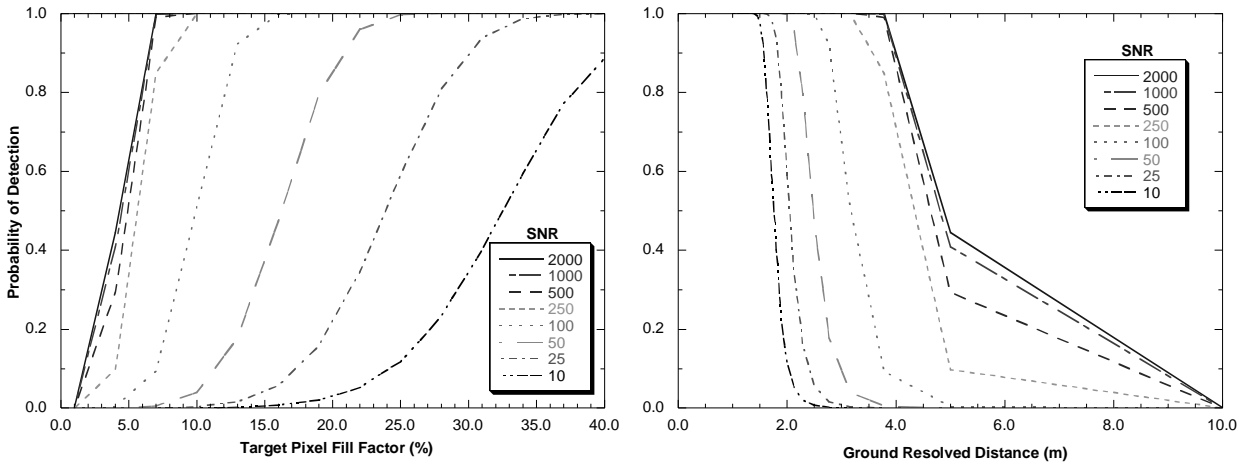


Figure 2. Model-predicted detection performance tradeoffs as fraction of pixel (left) and conversion to ground resolved distance for a 1 sq. m. target (right).

Figure 3 shows another example result plotting the detection probability versus ground resolved distance as a function of the number of spectral channels. Also shown in Figure 3 is our definition of constant performance. For each trade, we identified the triplet of parameters (GRD, number of channels, SNR) that achieved  $P_D = 0.8$  and  $P_{FA} = 10^{-5}$ . This criterion was selected as the metric for the constant performance concept introduced in Section 2. Figure 4 plots the resulting surface (for a single target/background pair) of model-derived results in a manner similar to the notional concept illustrated in Figure 1.

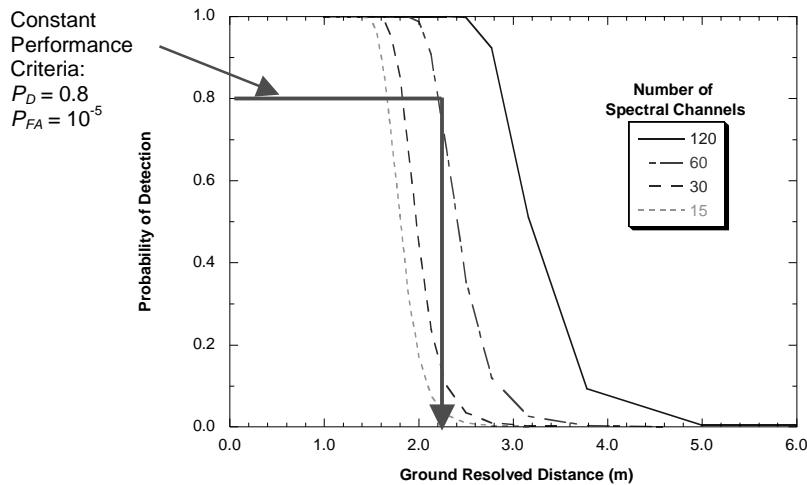


Figure 3. Model-predicted detection performance tradeoffs for number of channels and ground resolved distance.

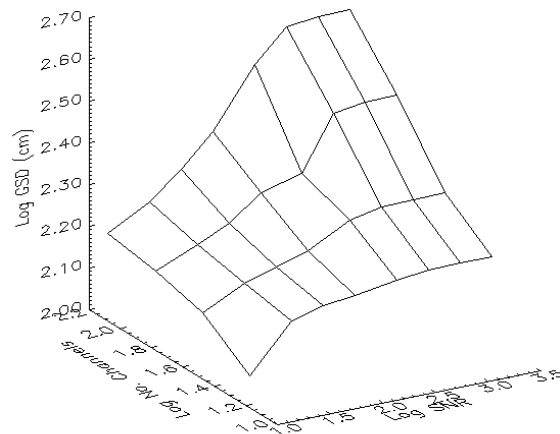


Figure 4. Example model-derived constant performance surface.

Note the values plotted Figure 4 are the logarithms of the actual parameter values. This transformation was done to achieve a more linear surface. These surfaces were calculated for all target/background combinations and a regression performed to a linear function of the transformed parameter values modeled after the NIIRS GIQE. The resulting SQE is shown in equation 2 where GRD represents the ground resolved distance in cm, SNR is the signal-to-noise ratio, and  $N$  is the number of channels in the reflective solar spectral region (0.4 to 2.5  $\mu\text{m}$ ).

$$SQRS = 9.65 - 3.22 \log_{10}[GRD(cm)] + 0.44 \log_{10}[SNR] + 0.81 \log_{10}[N] \quad (2)$$

In developing equation 2, we selected one significant constraint. Since the spectral resolution comes in through the specification of the number of channels  $N$  in the reflective solar region, the equation could mathematically be used to predict the SQRS for a single band panchromatic EO image by setting  $N = 1$ . Given that there is the established NIIRS scale for this case, it would seem useful to have the SQE predict similar values as the GIQE. This is also an intuitive constraint since a spectral image could be used to synthesize a panchromatic image by adding all spectral images together to form one panchromatic image. Another constraint we employed was to place the typical state of the art in airborne imaging spectrometers at about the middle of a 0 – 9 rating scale.

Given the SQE developed in this work, it is interesting to see how existing and hypothetical spectral imaging systems would be rated on the SQRS. Table 3 provides a summary of the parameters specified, the predicted SQRS and its standard deviation ( $\sigma$ ) based on the various target/background combinations. Also shown are the NIIRS values predicted by the GIQE for the cases where the number of channels,  $N$ , is equal to 1. Instrument names are shown for the cases where the parameter combinations correspond to an existing sensor. Examination of this table reveals the sets of instrument characteristics corresponding to the range of levels postulated under the SQRS.

Table 3. Example parameters and resulting model-based SQRS values, the SQRS standard deviation using the SQE derived from the various target/background combinations, the corresponding NIIRS value for cases where  $N=1$ , and the existing instrument where appropriate.

Input Parameters			Resulting Values				
<i>GRD</i> ( <i>m</i> )	<i>SNR</i>	<i>N</i>		<i>SQRS</i>	$\sigma_{SQRS}$	<i>NIIRS</i>	<i>Example Sensor</i>
30	100	6		-0.1	0.3		Landsat Thematic Mapper
20	100	4		0.4	0.3		SPOT Multispectral
10	100	1		0.9	0.5	0.7	SPOT Panchromatic
30	100	210		1.2	0.1		EO-1 Hyperion
20	500	224		2.1	0.1		AVIRIS at 20 km
8	100	210		3.0	0.1		Obview-4 Warfighter-1
1	100	1		4.1	0.5	4.0	
3	100	210		4.4	0.1		
1	100	6		4.7	0.3		
3	1000	210		4.9	0.1		
1	10	210		5.5	0.2		
1	100	210		6.0	0.1		
1	300	210		6.2	0.1		HYDICE at 2 km
1	1000	210		6.4	0.1		
0.5	100	210		6.9	0.1		
1.0	1000	2100		7.2	0.2		
0.1	100	1		7.3	0.5	7.3	
0.5	1000	210		7.4	0.1		
0.2	300	210		8.1	0.1		
0.1	1000	210		9.6	0.1		

## 5. EMPIRICAL TRADE STUDY AND SPECTRAL QUALITY EQUATION

While the model-based analysis provides a convenient and quick way to study the parameter sensitivities, it is prudent to consider a similar study using empirical data collected by a real sensor. Data collected by the HYDICE [9] airborne imaging spectrometer over forest and desert backgrounds, and similar objects as the model case, were analyzed. The various SQE's (one for each target/background pair) were derived from the detection results in a manner analogous to the model-based approach.

Several constraints of the empirical data restricted us from performing identical analyses to the model-based approach. In particular, the empirical data have sensor noise, artifacts, and residual calibration errors, which set an upper bound on the SNR. Since we add random noise to the data when performing the SNR sensitivity analyses, we limited the range of SNR studied to 25 – 100. In addition, the finite number of background samples in each image limited the false alarm rate used in the constant performance criterion to  $10^{-4}$ .

Table 4 shows a comparison between the SQRS values predicted by the model-based equations and those predicted by the empirical analyses for a range of parameter values. Note that since the false alarm rate supported by the empirical analyses was only  $10^{-4}$ , the model-based analyses were recomputed for this false alarm rate. As can be seen, the empirical-based SQRS values are lower than the model-based results, but the relative values track in a similar manner showing that the model-based results appropriately represent the sensitivity of spectral quality to the parameter combinations.

Table 4. Example parameters and resulting model-based SQRS values compared to the empirical-based SQRS means and standard deviations ( $\sigma$ ).

Notional Sensor Parameters			Model-based Result	Empirical-based Result	
<i>GRD (m)</i>	<i>SNR</i>	<i>N</i>	<i>SQRS</i>	<i>SQRS</i>	$\sigma_{SQRS}$
5	25	50	3.1	2.6	0.4
5	25	100	3.3	2.7	0.5
5	25	200	3.5	2.9	0.5
5	100	50	3.5	2.9	0.5
5	100	100	3.7	3.0	0.5
5	100	200	3.9	3.1	0.6
1	25	50	5.4	4.9	0.4
1	25	100	5.6	5.1	0.5
1	25	200	5.8	5.2	0.5
1	100	50	5.6	5.2	0.5
1	100	100	6.0	5.3	0.5
1	100	200	6.2	5.4	0.6
0.2	25	50	7.7	7.3	0.4
0.2	25	100	7.8	7.4	0.4
0.2	25	200	8.0	7.5	0.5
0.2	100	50	8.1	7.5	0.4
0.2	100	100	8.2	7.6	0.5
0.2	100	200	8.4	7.7	0.6

## 6. DISCUSSION AND FUTURE WORK

The studies presented in this paper represent one possible approach to the quantification of spectral image quality in the context of subpixel object detection. It is important to note that the results may have limited usefulness to applications outside of this context. The motivation for this approach was to develop a practical method so that insights may be gained for the larger, presently intractable, general concept of spectral image quality.

The approach developed here supports trends in parameter sensitivities that are intuitive and are supported by empirical analyses. The SQE developed provides a quantitative value by which comparisons can be made among spectral imaging systems and collapses to the well-established NIIRS in the limiting case of a single spectral channel.

Extensions of this concept are currently being explored for surface material identification and background terrain classification applications of spectral imagery. These applications have similar performance metrics (probability of correct identification and classification accuracy) to the detection problem studied here and lend themselves nicely to be studied in a similar manner.

## ACKNOWLEDGMENTS

The authors acknowledge support for this work by Mr. Ernie Reith and Mr. Wayne Hallada of the National Geospatial-Intelligence Agency. The authors would like to thank Capt. Paul Millhouse (USAF) for his thoughtful discussions on spectral quality metrics. Our colleague Kris Farrar (MIT/LL) is gratefully acknowledged for having performed the model runs used in this work. The HYDICE data used in the empirical analyses were supplied by the Spectral Information Technology Applications Center.

## REFERENCES

1. L. Martin, J. Vrabel, J. Leachtenauer, "Metrics for Assessment of Hyperspectral Image Quality and Utility," *Proceedings of International Symposium on Spectral Sensing Research*, 1999.
2. L. Bubion, K. Bennett, J. Bowles, and L. Martin, "Image Quality Evaluation of AOTF and Grating Based Hyperspectral Imaging Sensors," *Proceedings of International Symposium on Spectral Sensing Research*, 1999.
3. J. Sweet, J. Granahan, and M. Sharp, "An Objective Standard for Hyperspectral Image Quality," *Proceedings of AVIRIS Workshop*, Jet Propulsion Laboratory, Pasadena, California, 2000.
4. S. Shen, "Spectral Quality Equation Relating Collection Parameters to Object/Anomaly Detection Performance," *Proceedings of Algorithms and Technologies for Multispectral, Hyperspectral, and Ultraspectral Imagery IX*, SPIE Vol. 5093, 2003.
5. J. Leachtenauer and R.G. Driggers, *Surveillance and Reconnaissance Imaging Systems: Modeling and Performance Prediction*, Artech House, Inc., Norwood, MA, 2001.
6. J. Leachtenauer, "National Imagery Interpretability Rating Scales: Overview and Product Description," *ASPRS/ACSM Annual Convention and Exhibition Technical Papers*, Vol. 1, pp. 262-272, 1996.
7. J. Leachtenauer, W. Malila, J. Irvine, L. Colburn, and N. Salvaggio, "The General Image Quality Equation," *Applied Optics*, pp. 8322-8328, 10 November 1997.
8. J. Kerekes and J. Baum, "Spectral Imaging System Analytical Model for Subpixel Object Detection," *IEEE Transactions on Geoscience and Remote Sensing*, vol. 40, no. 5, pp. 1088-1101, May 2002.
9. L. Rickard, R. Basedow, E. Zalewski, P. Silverglate, and M. Landers, "HYDICE: An Airborne System for Hyperspectral Imaging," *Proceedings of Imaging Spectrometry of the Terrestrial Environment*, SPIE Vol. 1937, pp. 173-179, 1993.